Microchimica Acta (2021) 188: 244
https://doi.org/10.1007/s00604-021-04902-1

ORIGINAL PAPER

# Dual-mode aptasensor for simultaneous detection of multiple food-borne pathogenic bacteria based on colorimetry and microfluidic chip using stir bar sorptive extraction

Ming Wang[1] · Jin Zeng[1] · Jiaqi Wang[1] · Xiao Wang[1] · Ye Wang[2] · Ning Gan[1]

Received: 30 March 2021 / Accepted: 15 June 2021 / Published online: 6 July 2021


## Abstract

A dual-mode aptasensor using colorimetry and microfluidic chip (MC) together with stir bar sorptive extraction (SBSE) has been developed for firstly qualifying samples contaminated with *Vibrio parahaemolyticus* (V.P) and *Salmonella typhimurium* (S.T), then precisely determine both of them in positive samples. For this purpose, the aptamer-streptavidin encoded probes (Apt-SAEs) corresponding to different bacteria were prepared in advance. Then, a stir bar modified with 4-mercaptophenylboronic acid (MPBA) was made to extract bacteria together with Apt-SAE probes. The binding event of aptamer and target triggered the formation of two sandwich structures containing Apt-SAE, V.P or S.T. The concentration of bacteria could be enriched by 1000 times within 15 min to avoid long-time enrichment process. Finally, the stir bar was immersed in the 3,3′,5,5′-Tetramethylbenzidine (TMB)-$H_2O_2$ solution for color development. The color could be observed by naked eyes to judge whether the analytes were present. The colorless samples were judged to be negative. For the positive samples, the adsorbed encoded probes corresponding to different bacteria would be eluted from the stir bar and rapidly analyzed by the MC. Under the optimized conditions, 100 CFU/mL of V.P or S.T or both of them could be observed by colorimetry and 35 CFU/mL of them could be detected ($S/N = 3$) by the MC. The assay has significant application value for on-site screening and multiple detection of food-borne pathogenic bacteria.

**Keywords** Dual-mode · Aptasensor · Microfluidic chip · Colorimetry · Simultaneous detection · Stir bar sorption extraction

## Introduction

As it is well known, food-borne pathogens contamination poses a threat to human health worldwide through diet [1]. Some bacteria like *Vibrio parahaemolyticus, Salmonella typhimurium* are not allowed to be detected in food samples by the national standard of China [2]. Simultaneous determination of them is an important criterion for monitoring and reflecting the degree of bacteria contamination in aquaculture waters [3]. At present, many immunological and molecular biology technologies have been developed and applied in monitoring of pathogenic bacteria in aquaculture, such as enzyme-linked immunosorbent assay (ELISA) [4], polymerase chain reaction (PCR) [5], loop-mediated isothermal amplification (LAMP) [6], rolling circle amplification (RCA) [7], and gene microarray [8]. The above methods could bring reliable and accurate results. However, some of them are time-consuming, requiring expensive instruments or complex manipulations [9, 10]. Therefore, rapid identification and quantification of multiple food-borne pathogenic bacteria by convenient assays are essential to food safety monitoring.

In many test cases, the samples contaminated by target bacteria often accounted for a part of all samples. If all samples were brought back to the laboratory for precise quantification of various bacteria, it would lengthen the analytical time and be labor intensive [11]. Furthermore, it would reduce the timeliness for on-site supervision because the bacteria could grow geometrically within a few hours, thus would cause serious infection to aquatic products and lead to a large scale of deaths [12]. It was possible to solve the above problems by adopting dual-mode detection strategy. The strategy

✉ Ye Wang
wangye20140915@163.com

✉ Ning Gan
ganning@nbu.edu.cn

[1] Faculty of Material Science and Chemical Engineering, Ningbo University, Ningbo 315211, China

[2] Zhejiang Pharmaceutical College, Ningbo 315211, China

normally includes two methods to detect same samples [13, 14]. Generally, a rapid and convenient assay was used to judge positive samples containing food-borne pathogenic bacteria, and negative samples were not tested again. Then another method was used to precisely quantify various bacteria from positive samples. Thus, the dual-mode detection strategy could greatly improve the detection efficiency, timeliness and save time. For example, Wu [15] fabricated a bimodal aptasensor for the quantitative determination of *V. parahaemolyticus* through the combination of a fluorescent method and colorimetric method, based on platinum-coated gold nanorods (AuNR@Pt) probe. This analytical method could detect 10 CFU/mL by fluorescence mode and 75 CFU/mL V.P by colormetric mode. Wang et al. [16] has developed a fluorescent and colorimetric dual-channel assay for *E. coli* identification based on the OPD-$Cu^{2+}$ sensing system. Both the fluorescent and colorimetric assay have a good sensitivity, reporting LODs of 100 CFU/mL and 44 CFU/mL respectively. According to the above studies, it could be found the colorimetry was very suitable for rapid screening because of visualization and no need for professional instruments [17–19]. It was also found that many reported dual-mode assays for food-borne pathogenic bacteria focused on single analyte measurements. However, there are many kinds of pathogenic bacteria that could coexist in aquaculture waters. Therefore, it is necessary to qualify or quantify all of them simultaneously in one test. Microfluidic chip (MC) is an ideal high-throughput platform for multiple targets separation and detection [20]. It normally takes several minutes to finish tests and the injecting volume could be as low as nanoliter or picoliter. Recently, some studies have revealed that MC could play an important role in the detection of multiple food-borne pathogenic bacteria. Zhang et al. [21] developed a rapid and sensitive strategy for the simultaneous detection of *E. coli*, *L. monocytogenes*, and *S. Typhimurium* in artificially contaminated milk using microchip capillary electrophoresis (MCE) coupled with multiplex polymerase chain reaction (PCR). The levels of detection were as low as 82 CFU/mL for *E. coli*, 68 CFU/mL for *L. monocytogenes*, and 85 CFU/mL for *S. Typhimurium*. Luo et al. [22] developed a specific method using an aptamer probe combining with the duplex PCR and MC-LIF to detect *S. Typhimurium and P. aeruginosa*, the limits of detection ($S/N = 3$) were 15 CFU/mL for *S. Typhimurium* and 5 CFU/mL for *P. aeruginosa*. All the studies showed the MC methods combining with aptamer probes could provide an ideal platform for rapid and simultaneous identification of various bacteria with high efficiency. However, due to the injection volume of MC is normally as small as pL or nL, its sensitivity may be limited. Thus, it usually takes several hours for culturing the pathogenic bacteria or amplifying the signals before detection.

The stir bar sorption extraction (SBSE) which was originally developed at the end of 1990s, is a kind of simple and solvent-free sample preparation technology with high enrichment capacity, detection sensitivity, and reproducibility [23]. Therefore, SBSE method could be used to directly extract pathogenic bacteria in large volume of aquaculture water with high concentration rate. It could achieve the goal of direct detection without a previous culture process, and shorten the analytical time. With the above assumptions, we hoped to develop a dual-mode aptasensor based on colorimetry and MC method together with SBSE enrichment. The assay could be used for effective on-site screening and accurate quantification of pathogenic bacteria.

The strategy was designed as following: Firstly, *Vibrio parahaemolyticus* (V.P) and *Salmonella typhimurium* (S.T) were employed to testify the proof-of-concept. The specific preparation process of the aptamer-streptavidin encoded probes (Apt-SAEs) and detection process were shown in Scheme 1. The aptamer modified with biotin (aptamer(V.P)-biotin or aptamer(S.T)-biotin) was conjugated with streptavidin modified with horseradish peroxidase (streptavidin-HRP) to generate the Apt-SAEs probes through the specific binding between biotin and streptavidin. After then, a stir bar self-assembled with 4-mercaptophenylboronic acid (stir bar@MPBA) was employed to nonspecifically extract V.P or S.T or both of them in aquatic waters added Apt-SAE probes. It was reported that phenylboric acid (PBA) could bind to polysaccharides on the cell wall of bacteria, which achieved specific enrichment [24, 25]. Then, the specific binding event among the bacteria, MPBA and Apt-SAE would result in the formation of sandwich structure. The HRP on the sandwich complex could catalyze the chromogenic reaction of 3,3′,5,5′-Tetramethylbenzidine (TMB) and $H_2O_2$ to emit the signal visualized by naked eyes [26, 27]. The color depth could be used to judge or semi-quantify the existence of V.P or S.T or both of them. For the colorless negative samples, the test would be finished. While for positive samples, the Apt-SAE probes corresponding to different bacteria on the stir bar were eluted, separated, and determined by MC. According to the relationship between the signal intensity and the standard concentrations, the concentrations of V.P and S.T in the sample could be accurately quantified. The as-prepared aptasensor was then employed to detect several aquaculture waters with satisfied results.

## Experimental

### Materials and reagents

The oligonucleotide sequences (listed in Table S1) were purchased from Shanghai Sangon Biological Engineering Technology and Services Co., Ltd. (Shanghai, China). PBS

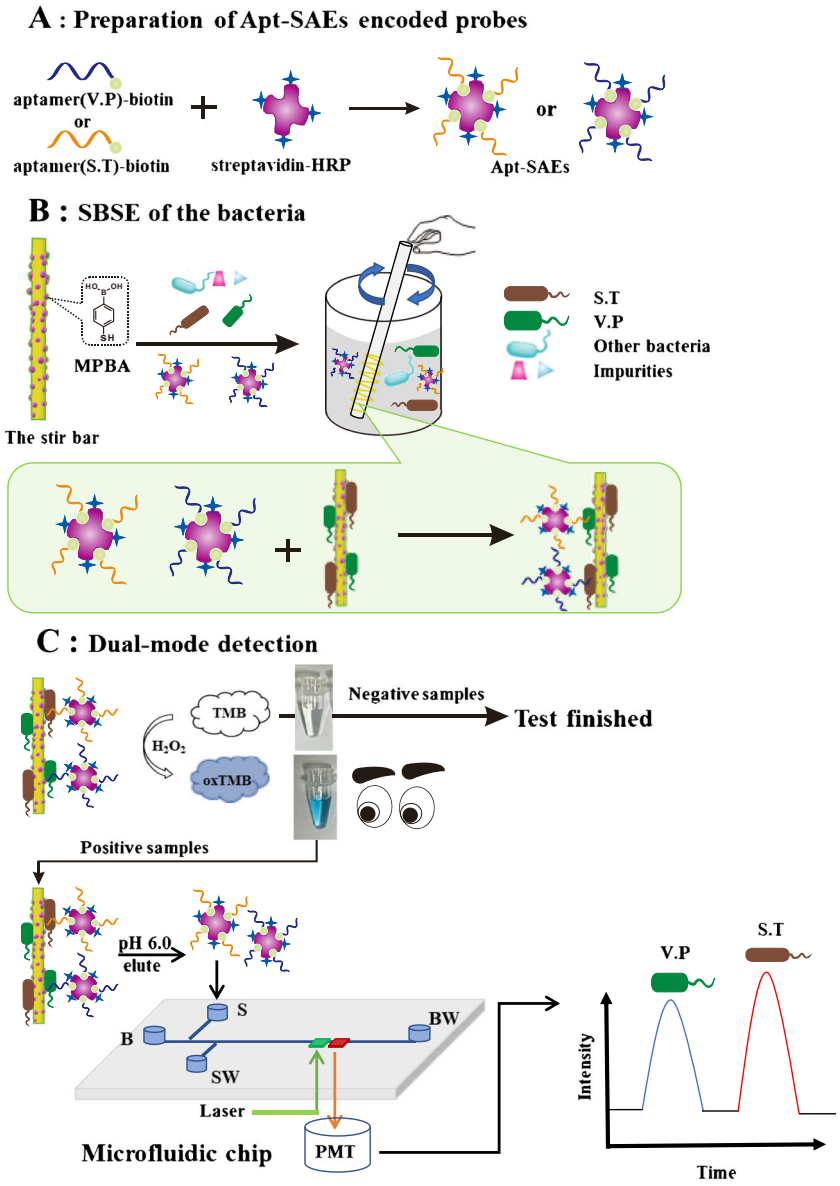


**Scheme 1** The mechanism of dual-mode aptasensor based on colorimetry and microfluidic chip for simultaneous detection of multiple food-borne pathogenic bacteria.

buffer (0.1 M phosphate buffered saline, 0.1 M KCl, pH 5–8) and binding buffer (1.0 M phosphate buffered saline, 10 mM EDTA, 250 mM NaCl, 20 mM $MgCl_2$, and pH 6–8) were prepared by standard methods. 3,3′,5,5′-Tetramethylbenzidine (TMB), 6-Mercapto-1-hexanol (MCH), HRP-conjugated Streptavidin, 4-mercaptophenylboronic acid (MPBA), hydrogen tetrachloroaurate (III) tetrahydrate ($HAuCl_4$), sodium citrate were from Sangon Biotechn Co., Ltd. (Shanghai, China). (3-mercaptopropyl)-Tri-Methoxysilane (MPTMS) was purchased from Signal-Aldrich Co., Ltd. (Milan, Italy). *Vibrio parahaemolyticus* (*V. parahaemolyticus*, ATCC 17802), *Salmonella typhimurium* (*S. Typhimurium*, ATCC 14028), *E. coli* (*E. coli*, ATCC 25922), *Staphylococcus aureus* (*S. aureus*, ATCC 29213), and *Listeria monocytogenes* (*L. M*, ATCC 13932) were obtained from Luwei Microbial Sci. and Tech. Co., Ltd. (Shanghai, China). The bare gold bar (99.99%, 25.0 cm in length and 0.2 mm in diameter) was obtained from Sinopharm Chemical Reagent Co. Ltd. (Shanghai, China). SYBR Gold (10000×) was obtained from Shimadzu Co, Ltd. (Tokyo, Japan). All of other chemicals were analytical grade and used without further purification. Double-distilled water was used throughout all this work.

Scanning electron micrographs (SEM) were obtained by using a S3400N scanning electron microscope from Hitachi Co, Ltd. (Tokyo, Japan). The UV-vis spectra were recorded by a UV-1800 spectrophotometer Shimadzu Co, Ltd. (Tokyo, Japan). MultiNA 202 system was purchased from Shimadzu Co, Ltd. (Tokyo, Japan).

### Preparation of Apt-SAEs encoded probes

The Apt-SAE encoded probes were prepared in advance, 50 mL PBS buffer (pH 7.4) containing 10 μM aptamer-biotin and 1.0 μM streptavidin-HRP solution was shaken on a shaker (120 rpm) at room temperature for 2 h to obtain Apt-SAE (1.0 μM).

### Preparation of the stir bar

Gold nanoparticles (AuNPs) were prepared by the citrate-reduction method [28]. Stir bar modified with AuNPs (stir bar@AuNPs) was synthesized according to literature [29]. The specific steps were shown in the supplementary S1. Subsequently, the 25.0 cm stir bar@AuNPs was incubated with MPBA (10 mM, 10 mL) solution at room temperature for 2 h. After the reaction, it was rinsed in PBS buffer (pH 7.4) three times, and then immersed in MCH (1.0 mM, 10 mL) solution for 2 h to block the unspecific adsorption sites. After the stir bar was rinsed three times with PBS, the preparation of the stir bar@AuNPs was completed.

### Colorimetric measurement

Binding buffer (50 mL, pH 8.0) and Apt-SAEs (50 mL, 1.0 μM) were added into a flask, and 400 mL aquaculture water containing the V.P and S.T (10, $1 \times 10^2$, $1 \times 10^3$, $1 \times 10^4$, $1 \times 10^5$, $1 \times 10^6$, and $1 \times 10^7$ CFU/mL) were added to the solution. During the extraction process, the stir bar wrapped around a glass rod was immersed in water samples (Fig. S1A), and stirred (100 rpm) at room temperature for 15 min. Then the stir bar was taken out and rinsed with PBS buffer (pH 7.4) three times to remove the unconjugated V.P, S.T and Apt-SAEs. Therefore, a three-sandwich structure of Apt-SAE, V.P or S.T, and stir bar was obtained. Finally, the stir bar with three-sandwich structure was immersed in 400 μL TMB and $H_2O_2$ solution to trigger the catalytic chromogenic reaction, and then its color change could be observed after 5 min. If its color turned blue, it meant that the sample contained at least one kind of bacteria.

### Quantitative detection of various bacteria by MC

For the positive samples, the stir bar with three-sandwich structure was immersed into the PBS buffer (400 μL, pH 6.0) and eluted for 20 min by shaking (100 rpm). The Apt-SAE encoded probes on the stir bar would release into the eluant. 150 pL of the eluent was injected into the sampling port of microfluidic chip (Fig. S1) by electrokinetic injection (7 s × 10 kV). The Apt-SAE in the eluate has fluorescence by adding (1×) SYBR gold to bind with DNA strands. The excitation wavelength was 495 nm and the emission wavelength was 537 nm. Then the samples containing eluted Apt-SAEs were separated and determined by the chip using the standard program providing by the Shimazu Co.Ltd. of MCE 202 MultiNA. The peaks at 65 s and 71 s were correspondent with Apt(V.P)-SAE and Apt(S.T)-SAE, respectively. The intensity of peak was employed for quantifying the target bacteria. After the analysis, the micro-channels of the MC were washed three times with water and the matching eluting buffer provided by Shimazu Co., Ltd.

### Detection of V.P and S.T in aquatic samples by the dual-mode aptasensor

The 400 mL water sample was collected from the area to be tested. The water samples were filtered through a 140 μm membrane to remove solid particles such as stone and dirt. Fifty milliliters binding buffer (pH 8.0, 1.0 M PBS) and 50 mL Apt-SAEs (1.0 μM) were added to the sample. After 15 min of incubation, the stir bar was eluted in 400 μL PBS buffer (100 mM, pH 6.0) for 20 min. Then, the sample was injected (sampling volume is 150 pL) and detected by the MultiNA 202 system, and the concentrations of V.P and S.T were calculated according to the signal intensity of Apt(V.P)-SAE (65 s) and Apt(S.T)-SAE (71 s), respectively.

## Results and discussion

### Characterization of SBSE method

The morphology of V.P and S.T were characterized by scanning electron microscope (SEM) in Fig. 1A and B, respectively. As could be seen the length of V.P was about 2.5 μm and the width of it was 550 nm. And the length and the width of S.T was about 1.8 μm and 850 nm, respectively. From Fig. 1C, it could be found the surface of the stir bar was smooth, while the morphology of stir bar@AuNPs was rough with many spherical particles (Fig. 1D). It meant many AuNPs were successfully immobilized on the stir bar, which could provide many active sites for 4-mercaptophenylboronic acid. In addition, Fig. 1E depicted the surface of the stir bar which successfully captured V.P and S.T. The S element was detected by energy-dispersive spectroscopy (EDS) on stir bar@AuNPs-MPBA, which proved that MPBA has been successfully modified on the stir bar (Fig. 1F).

### Feasibility verification of the dual-mode aptasensor

Figure 2A and B showed the feasibility of dual-mode aptasensor for simultaneous detection of V.P and S.T. As shown in Fig. 2A, distinctive bands of aptamer (V.P)-biotin (1.0 μM) appeared in lane 1. As could be seen from the figure, the band of V.P ($10^5$ CFU/mL) was almost blank (lane 2). When streptavidin-HRP (0.2 μM, 50 μL) was mixed with

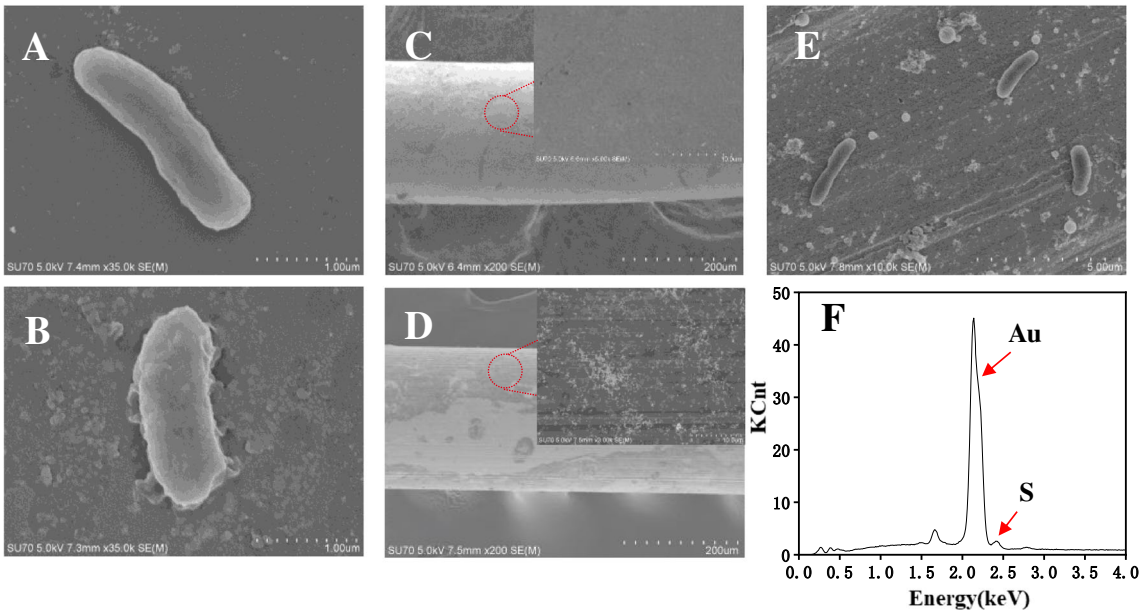


**Fig. 1** The SEM images of V.P (**A**), S.T (B), stir bar (**C**), stir bar@AuNPs (**D**), stir bar@ AuNPs-MPBA capturing V.P and S.T (**E**), EDS of stir bar@AuNPs-MPBA (**F**)

aptamer (V.P)-biotin (2.0 μM, 50 μL), a new lagged band appeared in lane 3. It meant that the Apt(V.P)-SAE probes were assembled successfully. Lane 4 showed the complex of Apt(V.P)-SAE and V.P. When Apt(V.P)-SAE was incubated with VP, the darkness of the band representing Apt(V.P)-SAE became lighter comparing with lane 2, and a new band appeared above the Apt(V.P)-SAE band. These proved that the Apt(V.P)-SAE was combined with V.P successfully. A similar phenomenon related to S.T also appeared in Fig. 2B. All these illustrated the feasibility of MC detection for V.P and S.T.

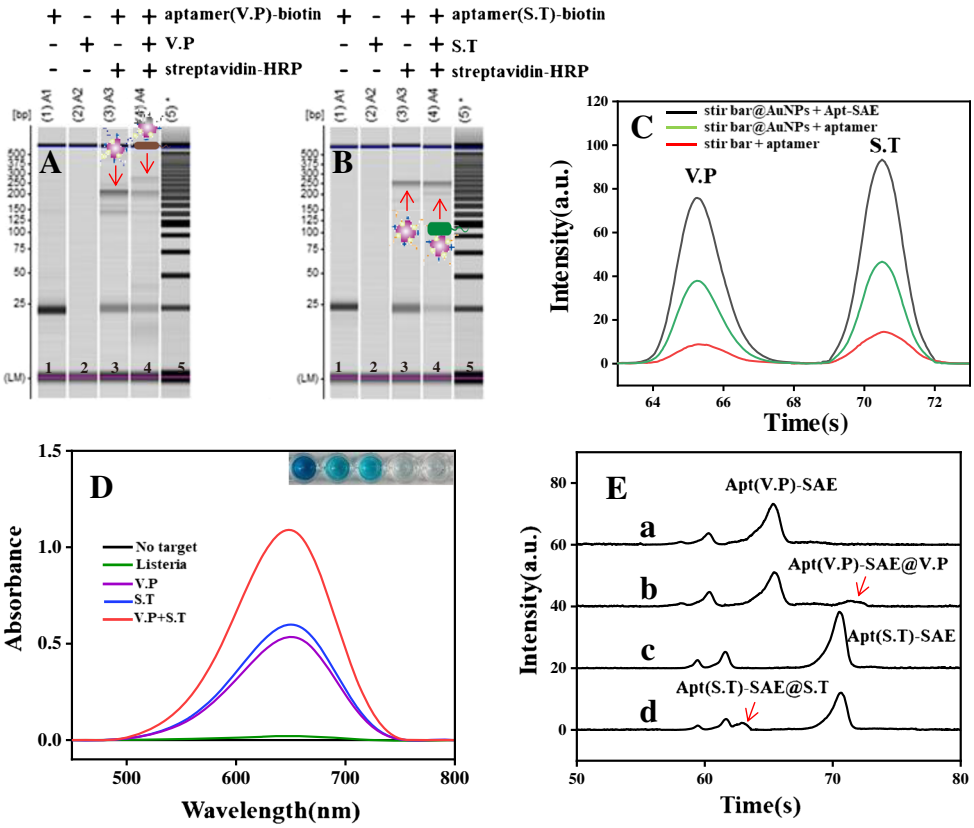


**Fig. 2.** **A** The electropherograms of Apt(V.P)-SAE and Apt(V.P)-SAE@V.P; **B** The electropherograms of Apt(S.T)-SAE and Apt(S.T)-SAE@S.T; **C** the amplification effect of AuNPs and Apt-SAE; **D** The feasibility of colorimetric visualization detection; **E** The feasibility of combining bacteria and Apt-SAE (excitation wavelength: 495 nm, emission wavelength: 537 nm)

At the same time, we studied the amplification effect of AuNPs on the stir bar and Apt-SAE encoded probes by MC. Gold nanoparticles (AuNPs) are widely used for color development with stable properties and controllable size. In addition, gold nanoparticles can also have strong bond cooperation with sulfhydryl and other groups [30], so 4-mercaptophenylboronic acid (MPBA) can be easily self-assembled on the surface of the stir bar to achieve functionalization. In Fig. 2C, the red curve depicted the sample containing V.P ($10^7$ CFU/mL) and S.T ($10^7$ CFU/mL) using aptamer and stir bar without AuNPs. The green curve reflected the results using aptamer and stir bar modified with AuNPs. The black curve depicted Apt-SAE and the stir bar modified with AuNPs. It could be clearly seen the signal increased gradually. The amplification factor was 10 times. The reasons were as following: AuNPs could obviously increase the specific area of stir bar and the amount of MPBA modified on it, which could extract and enrich low concentration of bacteria onto the stir bar. Thus, the extraction capacity of target bacteria could be increased largely compared with the stir bar without AuNPs. Moreover, it was well known that one streptavidin could bind up to four aptamer-biotin. Thus, one Apt-SAE probe was supposed to contain four aptamer, which was more capable of binding the target bacteria.

Figure 2D showed the feasibility of colorimetric detection. There were almost no absorption peaks from 400 nm to 700 nm in UV-vis spectrum when no target bacteria (black curve) or $10^7$ CFU/mL other bacteria (*Listeria monocytogenes*) existed (green curve). This meant that even if many bacteria could be adsorbed on the phenylboronic acid modified stir bar, the aptamer-streptavidin encoded probes (Apt-SAEs) could only combine with the target bacteria other than other interfering bacteria because the aptamer could only exhibit high affinity toward the target analyte. When $10^5$ CFU/mL V.P and S.T were incubated with the stir bar separately, the visible blue color could be observed by naked eyes and a strong characteristic absorption peak appeared at 650 nm (purple and blue curve). The reason was that the HRP on Apt-SAEs could catalyze the colorless 3,3′,5,5′-converting tetramethylbenzidine (TMB) into blue oxidized TMB (ox TMB) in the presence of $H_2O_2$ [31]. In addition, there was a stronger UV peak when $10^5$ CFU/mL V.P and S.T were simultaneously incubated with the probes than that from only $10^5$ CFU/mL V.P or S.T. The intensity of both V.P and S.T were almost same as the sum of their individual ones. The recovery was 95%. This meant the UV-vis spectrum could quantify the analytes.

Figure 2E showed the feasibility for simultaneous detection of V.P and S.T by the MC. The Apt(V.P)-SAE (0.1 μM) and Apt(S.T)-SAE (0.1 μM) were incubated with target bacteria ($10^5$ CFU/mL) separately in binding buffer (pH 8.0). It could be found that there were two obvious peaks in curve-a corresponding to Apt(V.P)-SAE while the concentration ratio of aptamer-biotin and streptavidin-HRP was 10 to 1. This was because a single streptavidin could bind one to four biotins, the multiple peaks represented different species of Apt(V.P)-SAE. The latter peak represented the 1:4 (streptavidin-HRP: aptamer-biotin) specie. The previous one maybe represented the 1:1 to 1:3 (streptavidin-HRP: aptamer-biotin) species. Even if 10 folds higher of aptamer-biotin were incubated with the streptavidin-HRP, there was also other species existed except 1:4 species. This could be due to that there were steric effects between aptamers while binding with the streptavidin. In the presence of V.P, the Apt(V.P)-SAE and V.P could form Apt(V.P)-SAE@V.P complex. So there was a new peak appeared which was corresponding to Apt(V.P)-SAE@V.P in curve-b and the peak intensity of Apt(V.P)-SAE was significantly reduced. Curve-c and curve-d showed the similar results of S.T. All of the above results proved that the MC could simultaneously and specifically detect V.P and S.T.

## Optimization of the experimental conditions

The experimental parameters including time of stir bar sorption extraction (SBSE) and desorption for Apt-SAEs on the stir bar, extraction and desorption pH for SBSE, concentration of $Mg^{2+}$ were optimized to achieve the best analytical performance. In the assay, the time for color reaction of TMB-$H_2O_2$ system was about 5 min, and that for MC was 3 min. Therefore, the pretreatment time by SBSE was the crucial factor for obtaining the largest signal response and shortest analytical time. $10^5$ CFU/mL V.P or S.T was used for the following experiment, and the number of experiments ($n$ = 5). From Fig. 3A, it could be seen that the colorimetric signal increased with the extraction time, and remained stable after 15 min. Thus, the optimal extraction time of SBSE was 15 min. The desorption time of Apt-SAEs from stir bar was also a key factor influencing the detection time by MC. After the stir bar extracted V.P or S.T together with the Apt-SAE encoded probes, the adsorbed probes were eluted by washing with PBS buffer (pH 6.0) and detected by MC. It could be seen that the MC signal increased with time and reached to a plateau at 20 min in Fig. 3B. As is well known that pH could affect the surface charge of bacteria and aptamer, then influenced the binding capacity of Apt-SAE toward the target bacteria. In this study, the pH values ranging from 6.0 to 8.0 were examined for extraction and detection by colorimetric method. The signal intensity reached to the maximum at pH 8.0 (Fig. 3C). The results were in consonance with that from Wang's group who employed pH 8.0 for incubating the aptamer with bacteria [32]. We employed pH 8.0 in further analysis. The desorption pH of Apt-SAE binding with the target bacteria on the stir bar was also optimized. The pH values of elution PBS buffer ranging from 5.0 to 8.0 were investigated. It could be found that pH 6.0 could completely elute the Apt-SAEs from the stir bar (Fig. 3D). It has been reported that the covalent bond of

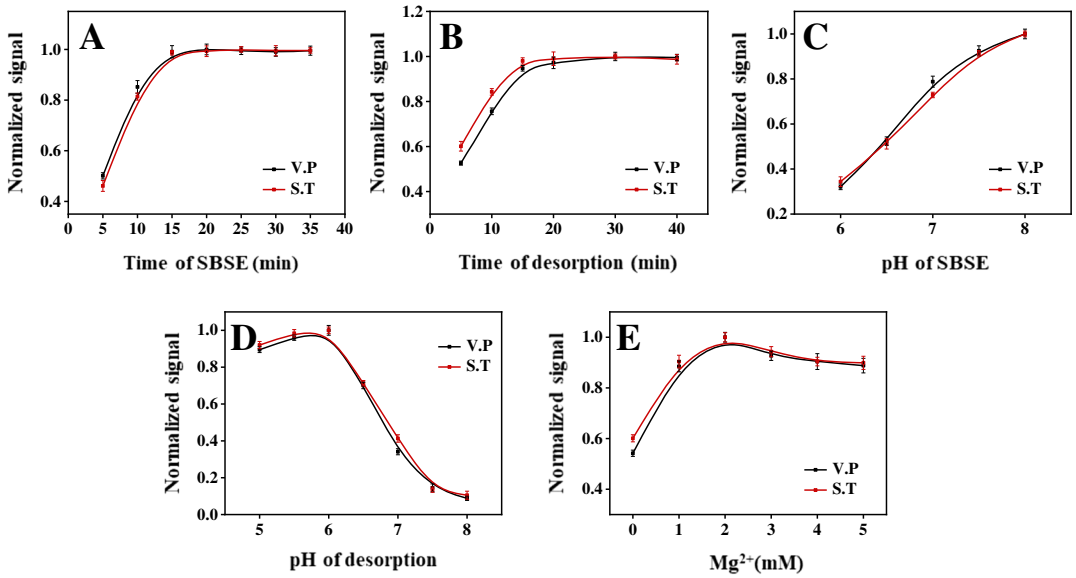


**Fig. 3** The samples contained $10^5$ CFU/mL V.P or S.T, $n = 5$ **A** the incubation time for SBSE, **B** the desorption time for target bacteria, **C** the pH of SBSE, **D** the pH of desorption, **E** concentration of $Mg^{2+}$, the experimental conditions were as follows: binding buffer (pH 8.0, 1 M PBS), eluent (pH 6.0, 100 mM PBS), incubation time (15 min), desorption time (20 min), and concentration of $Mg^{2+}$ (2.0 mM)

phenylboronic acid and 1,2–diol compound could be decomposed at pH 6.0 [33]. Thus, the MBPA on the stir bar maybe released the adsorbed bacteria at pH 6.0 and then the Apt-SAEs were released into supernatant.

$Mg^{2+}$ has been reported to play a prominent role on the binding capacity of aptamer to its target [34]. During the process of Apt-SAEs combining with the target bacteria, $Mg^{2+}$ aids in the formation of stable tertiary structures of aptamer, which is crucial for selective interaction between aptamer and

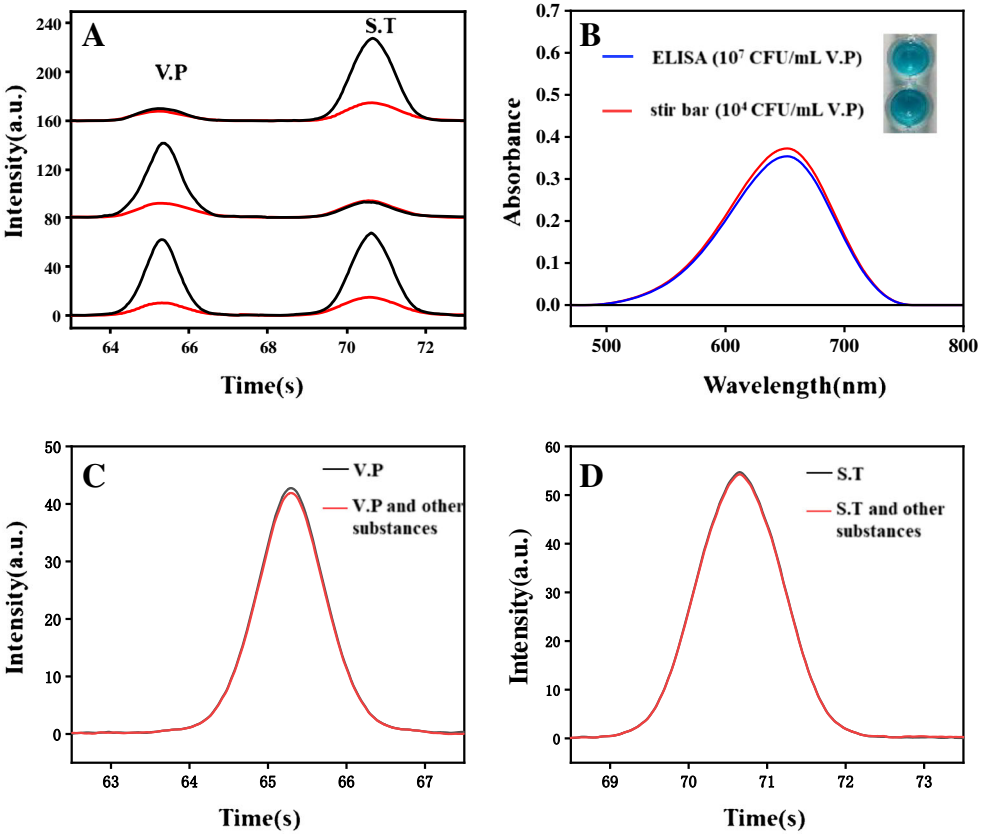


**Fig. 4** The cross-reactivity of V.P and S.T at different concentrations ($10^2$ and $10^6$ CFU/mL) by MC (**A**), the enrichment factor by SBSE (**B**), the interference of other substances ($10^5$ CFU/mL *Staphylococcus aureus*, $10^5$ CFU/mL *Listeria monocytogenes*, and $10^5$ CFU/mL *E. coli*, 0.16 g/L starch, 0.31 g/L agar) toward V.P (**C**), and toward S.T (**D**)

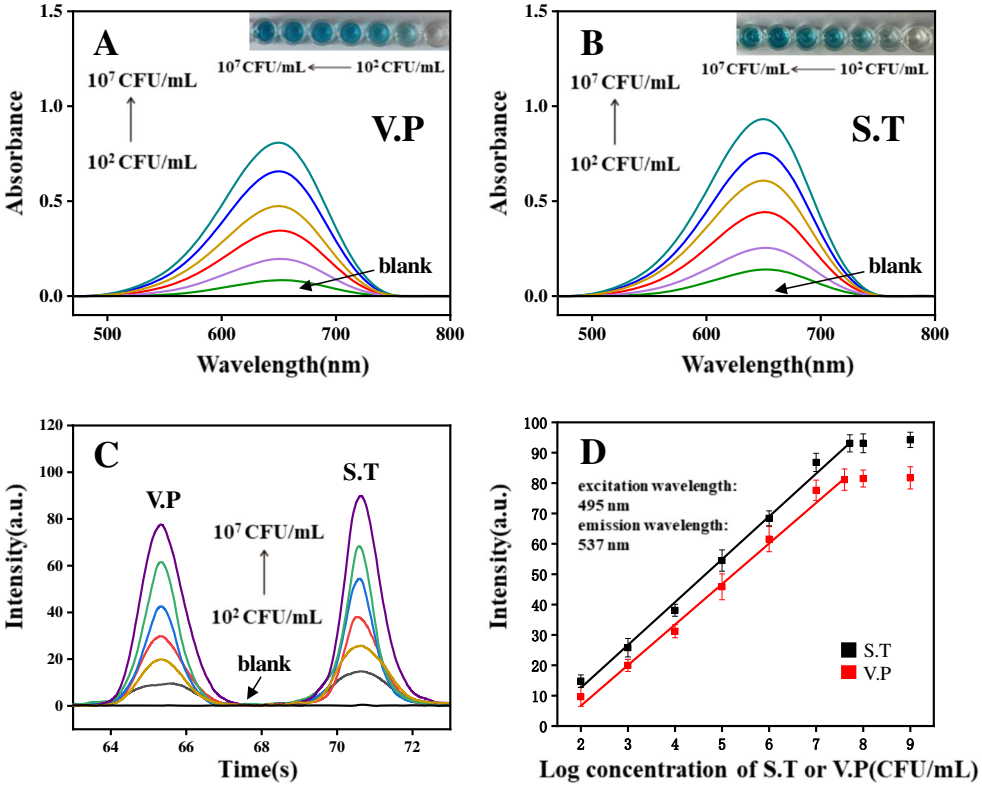


**Fig. 5** The colorimetric detection of **A** V.P and **B** S.T range from $10^2$ to$10^7$ CFU/mL; **C** The simultaneous detection of V.P and S.T range from $10^2$ to $10^7$ CFU/mL; **D** The calibration curve of the intensity for determination of V.P and S.T (excitation/emission wavelength: 495/537 nm), $n = 5$

their target [32]. In this study, we increased the $Mg^{2+}$ concentration of sample buffer from 0 mM to 5.0 mM. As shown in Fig. 3E, it revealed that the intensity reached to the maximum at 2.0 mM.

## Cross reactivity experiment and signal amplification

Under the optimum conditions, the cross reactivity of S.T and V.P in same samples was further studied. Each Apt-SAE probe own four aptamer DNA which could combine with SYBR Gold for signal development. The excitation wavelength was 495 nm and the emission wavelength was 537 nm. Because different Apt-SAEs embedded different length of aptamer, they could be separated by the microfluidic chip which was installed with polyacrylamide gel electrophoresis channels. Therefore, the Apt-SAEs corresponding to different target bacteria could be separated and detected by the microfluidic chip for simultaneously qualifying and quantifying different bacteria. As shown in Fig. 4, when the concentrations of V.P ($10^2$ CFU/mL) remained unchanged together

**Table 1** The comparison of methods to detect S.T and V.P

| Method | Detected bacteria | LOD (CFU/mL) | Linear range (CFU/mL) | Time (min) | Reference |
|---|---|---|---|---|---|
| Fluorescent aptasensor | S.Typhimurium | 25 | 50–$10^6$ | 40 | [35] |
| Colorimetric aptasensor | S.Typhimurium | 7 | 10–$10^6$ | 60 | [36] |
| Electrochemical | S.Typhimurium | 25 | 75–$7.5\times10^5$ | 60 | [37] |
| Electrochemical | *V. parahaemolyticus* | 2 | 2–$2.2\times10^8$ | 590 | [38] |
| Fluorescent aptasensor | V. Parahaemolyticus | 35 | 50–$10^6$ | 90 | [39] |
| Surface enhanced Raman light spectrum | V. Parahaemolyticus | 14 | $1.4\times10^2$–$1.4\times10^6$ | 90 | [40] |
| Fluorescent aptasensor | V. Parahaemolyticus | $5\times10^3$ | $3.4\times10^4$–$3.4\times10^7$ | 65 | [41] |
| | S.Typhimurium | $5\times10^3$ | $3.8\times10^4$–$3.8\times10^7$ | 65 | |
| Fluorescence resonance energy transfer | V. Parahaemolyticus | 25 | 50–$10^6$ | 150 | [42] |
| | S.Typhimurium | 35 | 50–$10^6$ | 150 | |
| Dual-mode aptasensor | V. Parahaemolyticus | 35 | $10^2$–$10^7$ | 40 | This |
| | S.Typhimurium | 35 | $10^2$–$10^7$ | 40 | work |

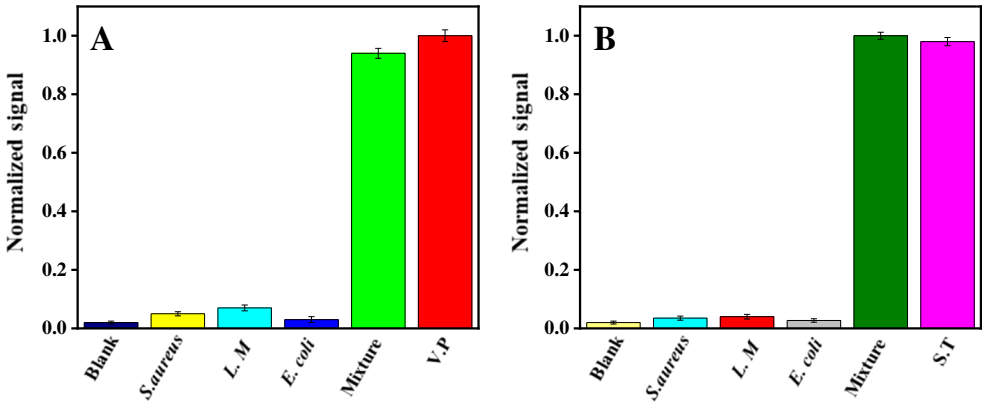


**Fig. 6** Specificity experiments of $10^5$ CFU/mL **A** V.P and **B** S.T with the existence of $10^7$ CFU/mL *Staphylococcus aureus*, *Listeria monocytogenes*, and *E. coli* ($n = 3$)

with different concentrations of S.T, the signal intensity of S.T was significantly increased from $10^2$ to $10^6$ CFU/mL, while the signal of V.P remained unchanged. Similarly, when the concentrations of S.T ($10^2$ CFU/mL) remained unchanged and different concentrations of V.P were added, the signal of V.P increased from $10^2$ to $10^6$ CFU/mL while that of S.T was stable. Upon the concentrations of S.T and V.P were increased, both signals enhanced accordingly. The above results indicated that there would be no cross-reactivity of two target bacteria, and the multiple assay could be employed.

The enrichment factor of SBSE was testified. The stir bar was used to enrich 400 mL sample containing V.P ($10^4$ CFU/mL) then eluted by PBS buffer (0.4 mL, pH 6.0). It could be seen from Fig. 4B, the colorimetric signal was as same as that by ELISA for sample containing $10^7$ CFU/mL V.P. All these probed that the enrichment factor by SBSE was about 1000 times, which could obviously increase the sensitivity of the assay.

The phenylboric acid on the stir bar was combined with the polysaccharides on the cell wall of bacterial, which realized the capture of the bacteria. However, other nontarget bacteria and polysaccharides in actual water could also be combined with phenylboronic acid, which would interfere with the experimental results. As shown in Fig. 4C, the black curve depicted the MC signal intensity of $10^5$ CFU/mL V.P in the absence of other impurities. The red curve depicted the MC signal intensity of $10^5$ CFU/mL V.P in the presence of other substances ($10^5$ CFU/mL *Staphylococcus aureus*, $10^5$ CFU/mL *Listeria monocytogenes*, and $10^5$ CFU/mL *E. coli*, 0.16 g/L starch, 0.31 g/L agar). It is not hard to see that the signal intensity of the two cases were almost the same. The conclusion of Fig. 4D was similar to that of Fig. 4C. It could be concluded that other bacteria and polysaccharides in the environment would not affect the testing results.

## The analytical performance for V.P and S.T

Under the optimum conditions, we evaluated the analytical performance of the dual-mode aptasensor toward S.T and V.P. S.T and V.P were diluted to different concentrations with PBS buffer ($1 \times 10^2$, $1 \times 10^3$, $1 \times 10^4$, $1 \times 10^5$, $1 \times 10^6$ and $1 \times 10^7$ CFU/mL), and then conducted further analysis. As showed in Fig. 5A and B, the UV-vis absorption peak intensity at 650 nm increased corresponding to the concentrations of V.P and S.T. The visible color could be observed (the insets in Fig. 5A and B). Therefore, the aptasensor could realize self-quantification for concentrations of V.P and S.T by naked eyes through the depth of color.

**Table 2** Detection of V.P in real samples by the dual-mode aptasensor ($n = 5$)

| Sample | Added | Detected by this method | Detected by standard method | Recovery of this method | RSD |
|---|---|---|---|---|---|
| V.P | (CFU/mL) | (CFU/mL) | (CFU/mL) | (%) | (%) |
| Water-1 | 0 | $(14.77\pm0.621)\times10^1$ | $(15.40\pm0.551)\times10^1$ | 95.9 | 4.2 |
| | $10^2$ | $(2.478\pm0.136)\times10^2$ | $(2.560\pm0.165)\times10^2$ | 96.8 | 5.5 |
| | $10^5$ | $(1.003\pm0.034)\times10^5$ | $(1.012\pm0.027)\times10^5$ | 99.1 | 3.4 |
| Water-2 | 0 | $(13.19\pm0.686)\times10^1$ | $(13.40\pm0.612)\times10^1$ | 98.4 | 5.2 |
| | $10^2$ | $(2.346\pm0.087)\times10^2$ | $(2.300\pm0.111)\times10^2$ | 102 | 3.7 |
| | $10^5$ | $(1.036\pm0.054)\times10^5$ | $(1.041\pm0.065)\times10^5$ | 99.5 | 5.2 |
| Water-3 | 0 | $(14.75\pm0.546)\times10^1$ | $(14.60\pm0.342)\times10^1$ | 101 | 3.7 |
| | $10^2$ | $(2.430\pm0.078)\times10^2$ | $(2.440\pm0.022)\times10^2$ | 99.6 | 3.2 |
| | $10^5$ | $(1.037\pm0.039)\times10^5$ | $(1.017\pm0.051)\times10^5$ | 102 | 3.8 |

**Table 3** Detection of S.T in real samples by the dual-mode aptasensor ($n$ = 5)

| Sample | Added | Detected by this method | Detected by standard method | Recovery of this method | RSD |
|---|---|---|---|---|---|
| S.T | (CFU/mL) | (CFU/mL) | (CFU/mL) | (%) | (%) |
| Water-1 | 0 | $(18.07 \pm 0.484) \times 10^1$ | $(18.40 \pm 0.462) \times 10^1$ | 98.2 | 2.7 |
| | $10^2$ | $(2.826 \pm 0.081) \times 10^2$ | $(2.860 \pm 0.121) \times 10^2$ | 98.8 | 2.9 |
| | $10^5$ | $(1.004 \pm 0.058) \times 10^5$ | $(1.026 \pm 0.082) \times 10^5$ | 97.9 | 5.8 |
| Water-2 | 0 | $(16.75 \pm 1.039) \times 10^1$ | $(17.20 \pm 0.634) \times 10^1$ | 97.4 | 6.2 |
| | $10^2$ | $(2.718 \pm 0.117) \times 10^2$ | $(2.740 \pm 0.165) \times 10^2$ | 99.2 | 4.3 |
| | $10^5$ | $(0.952 \pm 0.055) \times 10^5$ | $(0.976 \pm 0.043) \times 10^5$ | 97.5 | 5.8 |
| Water-3 | 0 | $(20.07 \pm 0.803) \times 10^1$ | $(19.80 \pm 0.565) \times 10^1$ | 101 | 4.0 |
| | $10^2$ | $(2.952 \pm 0.068) \times 10^2$ | $(2.960 \pm 0.049) \times 10^2$ | 99.6 | 3.5 |
| | $10^5$ | $(1.054 \pm 0.046) \times 10^5$ | $(1.033 \pm 0.068) \times 10^5$ | 102 | 4.4 |

Figure 5C showed the intensity of MC increased with an increase in V.P and S.T concentrations. The Apt-SAE intensity exhibited good linear relationship with the logarithm of V.P and S.T ranging from $1 \times 10^2$ to $1 \times 10^7$ CFU/mL. However, when the concentration of target bacteria in the sample was greater than $10^7$ CFU/mL, the MC signal intensity tended to be constant. It was indicated that the saturated extraction amount of VP on the stir bar is $1.6 \times 10^{10}$ CFU/bar, and saturated extraction amount of ST is $2.1 \times 10^{10}$ CFU/bar, respectively. The linear equation of V.P was $y = 13.45C_{v.p}$-19.80 ($R^2 = 0.9936$), the limit of detection (LOD) was evaluated to be 35 CFU/mL ($S/N = 3$). And the linear equation of S.T was $y = 14.27C_{s.t}$-16.28 ($R^2 = 0.9951$), the LOD was also 35 CFU/mL (S/N = 3). In addition, Table 1 listed some recent methods for detecting S.T or V.P. Compared with all the methods, the dual-mode aptasensor showed higher sensitivity and a wider detection range. It could realize the detection of multiple targets with lower LOD. Moreover, there were no report about dual-mode aptasensor being suitable for both on-site and lab analysis of target bacteria up to now.

## Evaluation of specific experiments

In order to evaluate the stability and specificity of the dual-mode aptasensor, several other pathogenic bacteria (*Staphylococcus aureus*, *Listeria monocytogenes*, and *E. coli*) were chosen for interference experiments. The concentrations of all four bacteria were $10^7$ CFU/mL. Figure 6A showed V.P ($10^5$ CFU/mL) exhibited a strong signal that was consistent with its own existence, while the response of other pathogenic bacteria was negligible. The specificity experiment of S.T ($10^5$ CFU/mL) was shown in Fig. 6B. The result also demonstrated that other bacteria did not interfere the measurement of S.T. Accordingly, the dual-mode aptasensor showed satisfied specificity.

## Application in aquatic samples

To further evaluate the feasibility and practical application performance of the dual-mode aptasensor by using real water samples, all the samples were spiked with different concentrations of V.P and S.T ($10^2$ CFU/mL, $10^5$ CFU/mL), respectively. And the recovery was tested in spiked samples. The experimental data were listed in Tables 2 and 3, the recoveries of samples spiked V.P were in the range of 95.9–102% with the RSD values at 3.2–5.5%. And the recoveries of spiked S.T were in the range of 97.4–102% with the RSD values at 2.7–6.2%. These results showed that the proposed method by detecting V.P and S.T simultaneously in water samples was effective.

# Conclusion

In this study, a dual-mode aptasensor based on colorimetry and microfluidic chip was firstly constructed together with SBSE for on-site visual analysis and laboratory confirmation of multiple food-borne pathogenic bacteria (*Vibrio parahaemolyticus* and *Salmonella typhimurium*). Compared with the related reported literature, this strategy showed several merits: Firstly, the stir bar was employed for extraction of target bacteria with high enrichment times. Thus, there was no requirement for long-time culture before detection, which greatly saved time and improved the detection efficiency. Secondarily, the aptamer-streptavidin encoded probes (Apt-SAEs) achieved dual transduction of colorimetric and microfluidic chip signals by the analytes, and exhibited multiple amplification effects, thus, improved the detection sensitivity. Thirdly, this strategy combined the advantages of both colorimetry and MC, which not only realized rapid on-site screening, but also realized the simultaneous quantification of multiple bacteria. Finally, this strategy had the potential to detect other food-borne pathogenic bacteria in food by using corresponding aptamer, which opened up a new path for the

sensitive and rapid detection of multiple bacteria in foods. But there were some limitations in strategy. The total time for pretreatment, incubation, desorption process, and detection of samples was as long as 1 h. Moreover, the MPBA modified stir bar could adsorb different kinds of bacteria which would compete with target bacteria. Thus, it would influence further enhancement of sensitivity. All these should be resolved in our future work.

**Supplementary Information** The online version contains supplementary material available at https://doi.org/10.1007/s00604-021-04902-1.

**Acknowledgements** This work was supported by the National Natural Science Foundation of China (21974074), Zhejiang Provincial Natural Science Foundation of China (LY19B050001, LY20B050004), Natural Science Foundation of Ningbo (2019A610184, 2019A610197), Zhejiang Province Public Welfare Technology Application Research Project (LGN18H300001, LGC20B050006, LGC19B070003), Zhejiang Provincial Top Discipline of Biological Engineering(Level A) (KF2019001), Basic Research Project of Key Laboratory of Guangzhou (202102100001) and K. C. Wong Magna Fund in Ningbo University.

## Declarations

**Competing interests** The authors declare that they have no competing interests.

**Conflict of interest** The authors declare that they have no competing of interests.

## References

1. Wang L, Shen X, Wang T, Chen P, Qi N, Yin BC, Ye BC (2020) A lateral flow strip combined with Cas9 nickase-triggered amplification reaction for dual food-borne pathogen detection. Biosens Bioelectron 165:112364
2. Paudyal N, Pan H, Liao X, Zhang X, Li X, Fang W, Yue M (2018) A meta-analysis of major foodborne pathogens in Chinese food commodities between 2006 and 2016. Foodborne Pathog Dis 15: 187–197
3. Liu N, Zou D, Dong D, Yang Z, Ao D, Liu W, Huang L (2017) Development of a multiplex loop-mediated isothermal amplification method for the simultaneous detection of Salmonella spp. and *Vibrio parahaemolyticus*. Scientific Reports 7:45601
4. Yu N, Wu J (2019) Rapid and reagentless detection of thrombin in clinic samples via microfluidic aptasensors with multiple target-binding sites. Biosens Bioelectron 146:111726
5. Vinayaka AC, Ngo TA, Nguyen T, Bang DD, Wolff A (2020) Pathogen concentration combined solid-phase PCR on supercritical angle fluorescence microlens array for multiplexed detection of invasive nontyphoidal Salmonella serovars. Anal Chem 92:2706–2713
6. Yuan H, Chao Y, Li S, Tang MYH, Huang Y, Che Y, Wong AST, Zhang T, Shum HC (2018) Picoinjection-enabled multitarget loop-mediated isothermal amplification for detection of foodborne pathogens. Anal Chem 90:13173–13177
7. Yao L, Ye Y, Teng J, Xue F, Pan D, Li B, Chen W (2017) In vitro isothermal nucleic acid amplification assisted surface-enhanced Raman spectroscopic for ultrasensitive detection of Vibrio parahaemolyticus. Anal Chem 89:9775–9780
8. Davis MA, Lim JY, Soyer Y, Harbottle H, Chang YF, New D, Orfe LH, Besser TE, Call DR (2010) Development and validation of a resistance and virulence gene microarray targeting Escherichia coli and Salmonella enterica. J Microbiol Methods 82:36–41
9. Shahrokhian S, Ranjbar S (2019) Development of a sensitive diagnostic device based on Zeolitic Imidazolate Frameworks-8 using Ferrocene–Graphene oxide as electroactive indicator for Pseudomonas aeruginosa detection. ACS Sustain Chem Eng 7: 12760–12769
10. Shi H, Trinh Q, Xu W, Zhai B, Luo Y, Huang K (2012) A universal primer multiplex PCR method for typing of toxinogenic Pseudomonas aeruginosa. Appl Microbiol Biotechnol 95:1579–1587
11. Zhang X, Tang Q, Mi T, Zhao S, Wen K, Guo L, Mi J, Zhang S, Shi W, Shen J, Ke Y, Wang Z (2018) Dual-wavelength fluorescence polarization immunoassay to increase information content per screen: applications for simultaneous detection of total aflatoxins and family zearalenones in maize. Food Control 87:100–108
12. Di H, Ye L, Neogi SB, Meng H, Yan H, Yamasaki S, Shi L (2015) Development and evaluation of a loop-mediated isothermal amplification assay combined with enrichment culture for rapid detection of very low numbers of Vibrio parahaemolyticus in seafood samples. Biol Pharm Bull 38:82–87
13. Li N, Zong S, Zhang Y, Wang Z, Wang Y, Zhu K, Yang K, Wang Z, Chen B, Cui Y (2020) A SERS-colorimetric dual-mode aptasensor for the detection of cancer biomarker MUC1. Anal Bioanal Chem 412:5707–5718
14. Song C, Li J, Sun Y, Jiang X, Zhang J, Dong C, Wang L (2020) Colorimetric/SERS dual-mode detection of mercury ion via SERS-active peroxidase-like au@AgPt NPs. Sensors Actuators B Chem 310:127849
15. Wu Z (2019) A dual-mode (Fluorometric and colorimetric) Aptasensor for Vibrio parahaemolyticus detection using multifunctional nanoparticles. Food Anal Methods 12:1577–1584
16. Wang C, Gao X, Wang S, Liu Y (2020) A smartphone-integrated paper sensing system for fluorescent and colorimetric dual-channel detection of foodborne pathogenic bacteria. Anal Bioanal Chem 412:611–620
17. Ren R, Cai G, Yu Z, Zeng Y, Tang D (2018) Metal-polydopamine framework: an innovative signal-generation tag for colorimetric immunoassay. Anal Chem 90:11099–11105
18. Ren R, Cai G, Yu Z, Tang D (2018) Glucose-loaded liposomes for amplified colorimetric immunoassay of streptomycin based on enzyme-induced iron(II) chelation reaction with phenanthroline. Sensors Actuators B Chem 265:174–181
19. Lai W, Wei Q, Xu M, Zhuang J, Tang D (2017) Enzyme-controlled dissolution of MnO2 nanoflakes with enzyme cascade amplification for colorimetric immunoassay. Biosens Bioelectron 89:645–651
20. Zhang Y, Luo F, Zhang Y, Zhu L, Li Y, Zhao S, He P, Wang Q (2018) A sensitive assay based on specific aptamer binding for the detection of Salmonella enterica serovar Typhimurium in milk samples by microchip capillary electrophoresis. J Chromatogr A 1534: 188–194
21. Zhang Y, Hu X, Wang Q (2020) Sensitive and specific detection of *E. coli*, *Listeria monocytogenes*, and *Salmonella enterica* serovar Typhimurium in milk by microchip electrophoresis combined with multiplex PCR amplification. Microchemical Journal 157:104876
22. Luo F, Li Z, Dai G, Lu Y, He P, Wang Q (1615) Simultaneous detection of different bacteria by microchip electrophoresis combined with universal primer-duplex polymerase chain reaction. J Chromatogr A 2020:460734
23. David F, Sandra P (2007) Stir bar sorptive extraction for trace analysis. J Chromatogr A 1152:54–69

24. Cordes DB, Gamsey S, Singaram B (2006) Fluorescent quantum dots with Boronic acid substituted Viologens to sense glucose in aqueous solution. Angew Chem 118:3913–3916
25. Liang L, Liu Z (2011) A self-assembled molecular team of boronic acids at the gold surface for specific capture of cis-diol biomolecules at neutral pH. Chem Commun 47:2255–2257
26. Zeng R, Wang J, Wang Q, Tang D, Lin Y (2021) Horseradish peroxidase-encapsulated DNA nanoflowers: an innovative signal-generation tag for colorimetric biosensor. Talanta 221:121600
27. Gao Z, Lv S, Xu M, Tang D (2017) High-index {hk 0} faceted platinum concave nanocubes with enhanced peroxidase-like activity for an ultrasensitive colorimetric immunoassay of the human prostate-specific antigen. Analyst 142:911–917
28. Song K-M, Cho M, Jo H, Min K, Jeon SH, Kim T, Han MS, Ku JK, Ban C (2011) Gold nanoparticle-based colorimetric detection of kanamycin using a DNA aptamer. Anal Biochem 415:175–181
29. Zeng J, Gan N, Zhang K, He L, Lin J, Hu F, Cao Y (2019) Zero background and triple-signal amplified fluorescence aptasensor for antibiotics detection in foods. Talanta 199:491–498
30. Ma N, Ren X, Wang H, Kuang X, Fan D, Wu D, Wei Q (2020) Ultrasensitive controlled release Aptasensor using thymine-hg(2+)-thymine mismatch as a molecular switch for hg(2+) detection. Anal Chem 92:14069–14075
31. Zhang X, Yang Q, Lang Y, Jiang X, Wu P (2020) Rationale of 3,3′, 5,5′-Tetramethylbenzidine as the chromogenic substrate in colorimetric analysis. Anal Chem 92:12400–12406
32. Zhang Y, Zhu L, He P, Zi F, Hu X, Wang Q (2019) Sensitive assay of Escherichia coli in food samples by microchip capillary electrophoresis based on specific aptamer binding strategy. Talanta 197: 284–290
33. Wannapob R, Kanatharana P, Limbut W, Numnuam A, Asawatreratanakul P, Thammakhet C, Thavarungkul P (2010) Affinity sensor using 3-aminophenylboronic acid for bacteria detection. Biosens Bioelectron 26:357–364
34. McCluskey K, Boudreault J, St-Pierre P, Perez-Gonzalez C, Chauvier A, Rizzi A, Beauregard PB, Lafontaine DA, Penedo JC (2019) Unprecedented tunability of riboswitch structure and regulatory function by sub-millimolar variations in physiological Mg2. Nucleic Acids Res 47:6478–6487
35. Duan N, Wu S, Chen X, Huang Y, Xia Y, Ma X, Wang Z (2013) Selection and characterization of aptamers against Salmonella typhimurium using whole-bacterium systemic evolution of ligands by exponential enrichment (SELEX). J Agric Food Chem 61:3229–3234
36. Yuan J, Tao Z, Yu Y, Ma X, Xia Y, Wang L, Wang Z (2014) A visual detection method for Salmonella Typhimurium based on aptamer recognition and nanogold labeling. Food Control 37: 188–192
37. Jia F, Duan N, Wu S, Dai R, Wang Z, Li X (2015) Impedimetric Salmonella aptasensor using a glassy carbon electrode modified with an electrodeposited composite consisting of reduced graphene oxide and carbon nanotubes. Microchim Acta 183:337–344
38. Teng J, Ye Y, Yao L, Yan C, Cheng K, Xue F, Pan D, Li B, Chen W (2017) Rolling circle amplification based amperometric aptamer/immuno hybrid biosensor for ultrasensitive detection of Vibrio parahaemolyticus. Microchim Acta 184:3477–3485
39. Duan N, Wu S, Ma X, Xia Y, Wang Z (2014) A universal fluorescent aptasensor based on AccuBlue dye for the detection of pathogenic bacteria. Anal Biochem 454:1–6
40. Duan N, Shen M, Wu S, Zhao C, Ma X, Wang Z (2017) Graphene oxide wrapped Fe3O4@au nanostructures as substrates for aptamer-based detection of Vibrio parahaemolyticus by surface-enhanced Raman spectroscopy. Microchim Acta 184:2653–2660
41. Duan N, Wu S, Yu Y, Ma X, Xia Y, Chen X, Huang Y, Wang Z (2013) A dual-color flow cytometry protocol for the simultaneous detection of Vibrio parahaemolyticus and Salmonella typhimurium using aptamer conjugated quantum dots as labels. Anal Chim Acta 804:151–158
42. Duan N, Wu S, Dai S, Miao T, Chen J, Wang Z (2014) Simultaneous detection of pathogenic bacteria using an aptamer based biosensor and dual fluorescence resonance energy transfer from quantum dots to carbon nanoparticles. Microchim Acta 182: 917–923